

Chapter 2

Outline of Atomic Modelling and Spectral Emission from Plasmas

To model the radiative behaviour of atomic species in laboratory or astrophysical plasmas, it is necessary to know a number of key fundamental properties of the atoms, ions and electrons, whose interactions contribute to the spectral emission. The population distribution amongst excited states of the atoms or ions is essential for both predictive spectrum line studies and analysis and therefore must be established. To do this we must take into account all the rate coefficients of every participating atomic process that contributes to the formation of the individual level populations. Since the atomic structure of the atoms and ions is essentially an infinite assembly of levels, it is generally necessary to make certain simplifying assumptions about the nature of the plasma being investigated in order to make the problem tractable. While this prejudices the results of such studies, it can provide a convenient starting point that allows us to focus on the most influential assumptions which should eventually result in convergence on the correct model. Certainly it is possible to include or exclude those assumptions that prove to be far removed from the reality of the conditions in the plasma in question. In the sections that follow, some of the common models are outlined and it is shown that the most appropriate atomic modelling approach is that of *Generalised Collisional Radiative Theory*. In addition, as background, a brief description is given of each of the most important fundamental atomic processes.

Their incorporation into ADAS provides derived atomic data whose applications are focused primarily on individual plasma studies.

2.1 Plasma Modelling

2.1.1 Thermodynamic Equilibrium

Consider a plasma consisting of atoms, ions and electrons with number densities N_i and N_e respectively, where i refers to the state of the atom or ion. Then, if the free electrons and ions are confined within the plasma and no radiation can escape, the system is said to be in *complete thermodynamic equilibrium*. In such circumstances, the atoms, ions and electrons establish equilibrium energy distributions at a particular temperature, and the rate of every individual reaction is balanced by the rate of its inverse reaction.

The electron speed distribution is then referred to as Maxwellian and is given by

$$f(v) = 4\pi \left(\frac{m_e}{2\pi kT_e} \right)^{3/2} v^2 \exp \left(\frac{-m_e v^2}{2kT_e} \right) \quad (2.1)$$

where m_e is the mass of an electron, k is Boltzmann's constant, and T_k is the plasma kinetic temperature. The photon energy distribution of the system is that of a *black body* corresponding to the radiation temperature T_k . Therefore, the radiation field energy density at frequency ν , per unit frequency interval, is given by

$$U(\nu) = \frac{8\pi h (\nu^3/c^3)}{\exp(h\nu/kT_k) - 1} \quad (2.2)$$

This is known as Planck's function, where c is the speed of light and h is Planck's constant.

The population distribution of excited states within an ion and between ionisation states can be obtained for the system by means of the Boltzmann and Saha-Boltzmann equations. These are,

$$\frac{N_i}{N_j} = \frac{\omega_i}{\omega_j} \exp \{ - (E_i - E_j) / kT \} \quad (2.3)$$

and

$$\frac{N_i^z}{N_e N_k^{z+1}} = \frac{\omega_i^z}{\omega_k^{z+1}} \frac{h^3}{2 (2\pi m_e kT_e)^{3/2}} \exp(I/kT_e) \quad (2.4)$$

respectively, where the superscript z refers to the z times ionised state and $z+1$ to the next higher ionisation stage. In addition, N_i , ω_i and E_i are the population density, statistical weight and transition energy of the level i and there are corresponding expressions for the level j and the level k of the $z+1$ times ionised state.

Complete Thermodynamic Equilibrium is never achieved in laboratory plasmas but may be closely approached in astrophysical plasmas, for example stellar interiors. This is principally because the radiation can usually escape before being reabsorbed, but also because the timescales to reach equilibrium are usually longer than the time taken for the plasma to change in temperature or density. These equilibrium timescales are described in more detail in sec. 2.1.2. Anticipating these results, we see that in general the electrons form a Maxwellian distribution of velocities. The external radiation field, in a real plasma, is unlikely to be a black body but it may be a diluted version of one, for example, in the solar corona.

The excited state populations, in natural and laboratory plasmas, can attain Boltzmann values, but are more likely to correspond to those of statistical balance. Statistical balance assumes that the sum of processes which populate a level can be equated to the sum of processes that depopulate that same level. If this is not so, the sum of these reaction rates defines a particle interaction term (see left hand side of eq. 2.5). This term denotes the integral over all velocities, of the rate of change of the electron distribution, due to collisions with other particles (McWhirter & Summers (1985)).

$$\int \left(\frac{\partial f(N_i^{+z}, \mathbf{v})}{\partial t} \right)_{int} d\mathbf{v} = \sum_j N_e N_j q_{j \rightarrow i} - \sum_j N_e N_i q_{i \rightarrow j} + \sum_j N_j A_{j \rightarrow i} + \dots \quad (2.5)$$

where $A_{j \rightarrow i}$ is the spontaneous radiative transition probability and $q_{i \rightarrow j}$ and $q_{j \rightarrow i}$ are the electron impact excitation and deexcitation coefficients respectively. Eq. 2.5 also contains similar products of rate coefficients with participating species densities for ionising collisions, proton collisions, recombination interactions etc.

We can formulate certain expressions which show the relationships between the reaction rate coefficients. For example, if we consider radiative transitions in our system, we can have

1. Spontaneous Radiative Decay

$$X_j^{+z} \rightarrow X_i^{+z} + h\nu \quad (2.6)$$

2. Photoabsorption

$$X_i^{+z} + h\nu \rightarrow X_j^{+z} \quad (2.7)$$

3. Stimulated Emission

$$X_j^{+z} + h\nu \rightarrow X_i^{+z} + 2h\nu \quad (2.8)$$

The spontaneous radiative transition probability mentioned above is also known as the Einstein A-coefficient and describes eq. 2.6. Similarly, there are Einstein coefficients to describe eq. 2.7 and eq. 2.8 which are denoted $B_{i \rightarrow j}$ and $B_{j \rightarrow i}$ respectively. The statistical balance of these,

$$N_i U(\nu) B_{i \rightarrow j} = N_j [U(\nu) B_{j \rightarrow i} + A_{j \rightarrow i}] \quad (2.9)$$

together with the assumption of complete thermal equilibrium, eq. 2.2 and eq. 2.3, allow us to derive the following connections between them.

$$\omega_i B_{i \rightarrow j} = \omega_j B_{j \rightarrow i} = \frac{\omega_j A_{j \rightarrow i}}{8\pi h\nu^3/c^3} \quad (2.10)$$

In what follows, we neglect the effects of photon induced transitions such as photoabsorption and stimulated emission. This is equivalent to saying that the plasmas with which we are concerned are optically thin. This is probably a valid assumption for the solar transition region and corona (Zirker (1981)).

Each of the individual processes in eq. 2.5 has an inverse and if their rates equate they are said to be in *detailed balance*. Reaction terms occur in the equation in these detailed balance pairs. In statistical balance the interaction term is zero. Therefore, the dominance of the collisional or radiative processes, in the plasma, is controlled by the interplay between the $N_e N_j q_{j \rightarrow i}$ and $N_j A_{j \rightarrow i}$ terms. This is directly influenced by the plasma electron density. The radiative transition probabilities are generally much larger than the collisional deexcitation coefficients. Therefore, N_e must become large enough to overcome this deficit for collisional processes to take control. It is clear that

for every statistical balance equation, for every level of an atom or ion, there is a fixed N_e where this is true. Above this critical density, the collision processes balance and the spontaneous part of eq. 2.5 becomes negligible in comparison. When this happens, the system is said to be in *local thermodynamic equilibrium* and this is usually denoted LTE (note that the definition of LTE varies between authors and in the case of stellar atmospheres it is usual to define LTE by assuming that the population densities, opacity, emission and thermodynamic properties of a small volume of atmospheric material are the same as the thermodynamic equilibrium values, but at the *local* temperature and electron density (Mihalas (1978)).

In LTE the populations follow the distributions specified by the Boltzmann and Saha-Boltzmann equations. In reality, plasmas are more likely to be in LTE than complete thermodynamic equilibrium. The large cross-sections for collisional transitions between highly excited states makes this a strong possibility at least for them. In these circumstances, it is useful to modify eq. 2.4 by a b factor which gives a measure of the departure from LTE (McWhirter & Summers (1985)). Low lying levels are normally only close to, or in, LTE at extremely high densities. LTE can therefore be viewed as the high density collision dominated behaviour of plasmas. At low density the plasma is radiation dominated and a separate model is required for this regime.

One such model is that of *Coronal Equilibrium*. This is so named because it approximates the behaviour of the solar corona. The assumption is that atoms and ions are excited by electron collisions,



and that they deexcite by spontaneous radiative decay (eq. 2.6). They are collisionally ionised by electron impact,



and recombine also by electron collision,



This model is reasonable if the plasma is of low density and optically thin. The low density ensures that the spontaneous radiative term is greater than the collisional

deexcitation term. In addition, the fact that photons can escape without further interactions ensures that upward radiative transitions (e.g. photoabsorption) can be neglected. Essentially the model predicts that atoms and ions are excited by electron impact, and that they then have time to decay, by photon emission, before they are involved in any other reaction. Similarly, if an atom or ion is ionised, it has time to recombine before further disruptions.

As mentioned above, highly excited states could well be in LTE. This happens above what is termed the *collision limit*, \bar{i} say, where the excited state populations are dominated by collisionally induced transitions. States above \bar{i} effectively become part of the continuum due to their large cross-sections for transitions to neighbouring states (Burgess(1965) - unpublished, Jordan(1969)). Even at low density this is the case. At increasing density more and more states are in LTE and the collision limit is lowered. It is possible to extend the applicability of the coronal model if we treat ionisation and recombination as including transitions between levels below \bar{i} and levels above \bar{i} . This requires more detailed examination of intermediary states for step-wise ionisation and dielectronic recombination. Discussion of this is deferred until sec. 2.2.2.

We could pose a number of questions. For example, at what densities do collisional processes begin to dominate over radiative ones? At which excited state do collisional processes become important? When does it become necessary to take account of secondary processes that collisionally redistribute the populations before they have time to relax? It is concerns like these that have led to a reevaluation of the different modelling approaches. We wish to adopt an approach which deals with these issues.

2.1.2 Equilibrium Timescales

It is of interest to investigate the different relaxation timescales for the excited states of an atom or ion in a plasma. A comparison of these for low lying levels and highly excited ones, and also with plasma diffusion, transient event and instrument sampling times, enables us to determine our modelling approach. For example, do the low lying levels relax into equilibrium quicker than we can take readings with our instruments?

If so, is there any point in modelling them dynamically? It is interesting also to see whether the plasma itself has time to relax properly. How close is the plasma to thermodynamic equilibrium? Do the electrons generally have time to adopt a Maxwellian velocity distribution? Can we say that the electrons and protons have the same temperature?

First, let us look at these particle-particle equilibration timescales. McWhirter & Summers (1985) provide expressions for these, following the work on encounters between charged particles developed by Spitzer (1956). For a particle of mass m the self collision time is given by,

$$\tau_{sc}c = 0.12 \frac{1}{\alpha c a_0^2} \left(\frac{m}{m_e}\right)^{1/2} \left(\frac{kT_e}{I_H}\right)^{3/2} \frac{1}{N z^4 \ln \Lambda} \quad (2.14)$$

which gives us the following rough estimate for the electron-electron equipartition time.

$$\tau_{ee} \sim \frac{1.96 \times 10^7}{(cm^3 s^{-1})} \left(\frac{kT_e}{I_H}\right)^{3/2} \frac{1}{N_e \ln \Lambda} \quad (2.15)$$

Likewise, the proton-proton equipartition time follows from this due to the $(m_p/m_e)^{1/2}$ mass factor,

$$\tau_{pp} \sim \frac{8.43 \times 10^8}{(cm^3 s^{-1})} \left(\frac{kT_p}{I_H}\right)^{3/2} \frac{1}{N_p z^4 \ln \Lambda} \sim 43\tau_{ee} \quad (2.16)$$

McWhirter & Summers also gave an expression for the equilibration timescale between two different particles, viz.

$$\tau_{eq} = 0.0529 \frac{1}{\alpha c a_0^2} \frac{m_1 m_2}{m_e m_e} \left(\frac{kT_1 m_e}{I_H m_1} + \frac{kT_2 m_e}{I_H m_2}\right)^{3/2} \frac{1}{n^2 z_1^2 z_2^2 \ln \Lambda} \quad (2.17)$$

which leads to the approximate form for proton-electron thermalisation,

$$\tau_{ep} \sim \frac{8.64 \times 10^6}{(cm^3 s^{-1})} \frac{m_p}{m_e} \left(\frac{kT_e}{I_H} + 5.4 \times 10^{-4} \frac{kT_p}{I_H}\right)^{3/2} \frac{1}{n_p \ln \Lambda} \sim 1849\tau_{ee} \quad (2.18)$$

In eqs. 2.14 to 2.18, α is the fine structure constant, a_0 is the first Bohr radius, c is the speed of light, k is Boltzmann's constant, I_H is the first ionisation potential of the hydrogen atom and $\ln \Lambda$ is the coulomb logarithm which generally takes a value ~ 20 .

	$N_e(cm^{-3})$	$T_e(K)$	$\tau_{ee}(s)$	$\tau_{ii}(s)$	$\tau_{ie}(s)$
solar corona	$\sim 5 \times 10^8$	$\sim 1 \times 10^6$	~ 0.18	~ 8	$\sim 153 \rightarrow 348$
laboratory	$\sim 1 \times 10^{13}$	$\sim 1 \times 10^7$	$\sim 3 \times 10^{-4}$	1.3×10^{-2}	$\sim 0.3 \rightarrow 0.6$

Table 2.1: Relaxation timescales for selected plasmas

Table 2.1 gives values for these three timescales, using eq. 2.14 to 2.18, by taking typical values of electron density and temperature for the solar corona and a laboratory fusion plasma. For equipartition we have assumed that the electron contribution is dominant. In a fusion laboratory plasma the confinement time is of the order $\sim 1s$. In the solar corona, the plasma is generally assumed to be in a global steady state, although there are localised dynamic events. This last assumption is likely to be reevaluated as a consequence of the initial results from SOHO, as we shall see in later chapters. However, it appears that in both cases the electron velocities are indeed that of a Maxwellian distribution. Furthermore, they will have had time to thermalise before the ions have. It is likely that in both situations the ions will also thermalise, but in a laboratory plasma the equipartition of energy between ions and electrons does not necessarily have time to take place. Therefore, in a lab. plasma, a two temperature treatment is probably appropriate. This is also true for dynamic activity in the solar corona, but is not necessarily the case if we just consider the overall picture.

Turning now to the relaxation times for the excited states of the ions themselves. These timescales determine the lifetimes of the excited states and as such, influence our modelling approach. We can make simple ‘order of magnitude’ estimates of the relaxation timescales for ordinary excited states. Essentially this is the inverse of the sum of the transition probability and the product of electron density and the collisional rate coefficient i.e.

$$\tau_{ord} \sim \frac{1}{(N_e q_{i \rightarrow j} + A_{j \rightarrow i})} \quad (2.19)$$

This is dominated by the fastest reaction rate between the two levels. Usually this is the radiative transition probability which is typically very large compared to the

collisional rate coefficient. McWhirter & Summers (1985) give an approximate form for the radiative transition probability which reduces to $A_{j \rightarrow i} \sim 10^8 z 1^4$, where $z 1 = z + 1$. Therefore, the lifetime for an ordinary excited state is approximately,

$$\tau_{ord} \sim \frac{10^{-8}}{z 1^4} \quad (2.20)$$

Evidently, the lifetime of the ground state is dominated by collision processes since it has no possibility of radiatively decaying. In this case we should include ionisation and recombination coefficients in eq. 2.19, but we should exclude the transition probability term. In this case, the dominant reaction rate is that involving the excitation rate coefficient. McWhirter & Summers (1985) also give an approximate form for the excitation rate coefficient which reduces to $q_{i \rightarrow j} \sim 10^{-8}/z 1$. The lifetime is then inversely proportional to the electron density and can be approximated thus,

$$\tau_g \sim \frac{10^8 z 1}{N_e} \quad (2.21)$$

It is possible also to have metastable states whose lifetimes are comparable to the ground state. These are discussed in more detail in sec. 2.2.2 but arise principally due to their small radiative transition probabilities. Radiative decay from them is less likely as the only pathways from them to the ground state are via quantum mechanically forbidden transitions. Metastables can be influenced by recombination and ionisation processes, and despite their longevity will eventually decay to the ground level at low electron density. Eq. 2.19 for metastables would be similar to that for the ground state but with the spontaneous term reactivated. Once again the interplay between the dominance of the collisional and radiative terms is important. The influence of electron density means that metastable states will have long lifetimes at low density, but that above some threshold, the time constant will become dependent on density. They can therefore be viewed as a separate level grouping, midway between ground and excited states.

A final class of excited states to be considered are those that autoionise (sec. 2.2.1). These have extremely short lifetimes ($\sim 10^{-12} s$) and as such are related to the ordinary excited state and metastable state relaxation timescales as,

$$\tau_{auto} \ll \tau_{ord} \ll \tau_g \quad (2.22)$$

In general, the key lifetimes mentioned above will satisfy the following relationship also,

$$\tau_{met} \sim \tau_g \sim \tau_{plasma} \sim \tau_{ion} \gg \tau_{ord} \gg \tau_{ee} \quad (2.23)$$

where τ_{plasma} refers to plasma diffusion and dynamic timescales, and τ_{ion} refers to the ionisation relaxation timescale. A more detailed discussion of the latter is given in chap.2.

From these heuristic estimates a number of properties of the plasma are evident. We have established that the electron velocity distribution is very likely Maxwellian. It is also clear that the dominant populations of the atoms and ions will be in the ground and metastable states. Their lifetimes are comparable to plasma dynamic timescales and may be shorter than that necessary to establish ionisation equilibrium. As a result, these should be modelled dynamically via the equations of plasma transport (sec. 6.1.1). It is possible to make a separation of states between those that must be modelled in this way, and ones whose relaxation times are so short that they are already in equilibrium. The ordinary excited states and autoionising states fall into the latter category. We call this a *quasi-static separation of excited states* and refer to the highly excited states as being in *quasi-equilibrium*. This division of atomic states, between quasi-static and dynamic populations, allows us to separate the atomic modelling tasks. We can first calculate the excited state populations, emission functions and effective source coefficients. These can then be entered into a dynamical transport model. The spatial and temporal non-equilibrium model can then be advanced, and the new populations reassociated with the quasi-static state emission functions at a new local temperature and density. We require to derive a connection between the dynamic populations and the quasi-static ones that will provide us with these effective source coefficients. This leads us neatly into the approach we will adopt, that of *Collisional-Radiative Modelling*. We defer discussion of this until sec.2.2.2.

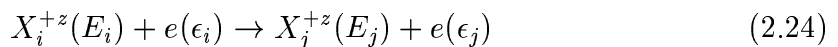
2.2 Radiating characteristics of plasmas

2.2.1 Relevant Atomic Processes

To complete our preparations it is necessary to discuss the reactions that we include in our atomic model. The assumption is made that we are dealing with a fully ionised hydrogen plasma. This is usually the case for both astrophysical and fusion plasmas. It therefore consists of electrons, protons, hydrogen atoms and minor species. Protons in this context refer to hydrogen ions of any isotope. The minor species are other elements in various stages of ionisation. It is the latter which contribute the greatest to the radiation emission and it is reactions involving these that must be considered. Despite this, we can neglect reactions between the minor species on the grounds that they occur too infrequently. Many body collisions, e.g. multiple ionisation, are also unlikely to be effective in the present context although they may be important for higher densities. We make special reference to three-body recombination here due to its influence on the generalised dielectronic recombination coefficients at low temperature and high density (see chap.4). We discuss the atomic processes in inverse pairs where appropriate.

Collisional Excitation/Deexcitation by Electron/Proton Impact

Consider the electron impact excitation reaction between two excited levels i and j , of an ion X^{+z} , of an element X ;



where E_i (E_j) is the excitation energy of level i (j), and ϵ_i (ϵ_j) is the incident (scattered) electron energy. This reaction will take place if $\epsilon_i \geq \Delta E_{ij}$, where $\Delta E_{ij} = E_j - E_i$. The reaction, (2.24), is described by a cross-section, $\sigma_{i \rightarrow j}(\epsilon_i)$, which is the effective target size of the ion that the electron has to hit. More completely, we can define the cross-section as follows. If we consider a flux of electrons, $f = N_e v_e$, incident on the ion with number density, N_i , then the number of electrons scattered into a small solid angle, $d\omega$, per unit time is $f N_i \sigma d\omega$. The differential cross-section is the

proportionality factor, σ , which is a function of the scattering angle, and the total cross-section is this integrated over all solid angles.

The symmetrical dimensionless quantity, Ω_{ij} , is the collision strength and it is related to the excitation and de-excitation cross sections by,

$$\Omega_{ij} = \left(\frac{\sigma_{i \rightarrow j}(\epsilon_i)}{\pi a_0^2} \right) \omega_i \left(\frac{E_i}{I_H} \right) = \left(\frac{\sigma_{j \rightarrow i}(\epsilon_j)}{\pi a_0^2} \right) \omega_j \left(\frac{E_j}{I_H} \right) \quad (2.25)$$

where $\omega_i(\omega_j)$ are the statistical weights of the lower (upper) level, πa_0^2 is the atomic unit of cross-section ($= 8.7974 \times 10^{-17} \text{cm}^2$) and I_H is the Rydberg unit of energy ($= 13.6058 \text{eV}$). When considering reaction kinetics in plasmas the effective collision strength is often used, and this is a function of Ω_{ij} such that,

$$\Upsilon_{ij} = \int_0^\infty \Omega_{ij}(\epsilon_j) \exp(-\epsilon_j/kT_e) d(\epsilon_j/kT_e) \quad (2.26)$$

for excitation from level i to level j at electron temperature T_e , where k is Boltzmann's constant and ϵ_j is the scattered electron energy after excitation. Υ_{ij} is sometimes also written as γ_{ij} . The excitation rate coefficient for this transition can also be obtained from the effective collision strength, viz.,

$$q_{i \rightarrow j}^e(T_e) = 2\pi^{1/2} \alpha c a_0^2 \left(\frac{I_H}{kT_e} \right)^{1/2} \frac{\Upsilon_{ij}}{\omega_i} \exp(-\Delta E/kT_e) \quad (2.27)$$

where α is the fine structure constant, c is the velocity of light and $2\pi^{1/2} \alpha c a_0^2 = 2.1717 \times 10^{-8} \text{cm}^3 \text{s}^{-1}$. The de-excitation rate coefficient can be calculated from detailed balance,

$$q_{j \rightarrow i}^e(T_e) = q_{i \rightarrow j}^e(T_e) \frac{\omega_i}{\omega_j} \exp(\Delta E/kT_e) \quad (2.28)$$

The various approximate forms and asymptotic behaviours, for the different transition types, are discussed in more detail in sec.3.1.4.

A similar excitation reaction takes place involving protons,

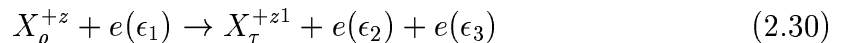


In general, electrons are more effective than protons at causing collisional transitions due to their larger reaction rate coefficients. These coefficients are products of the

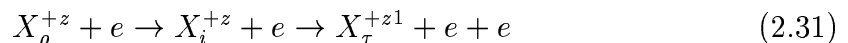
collision cross-section and the velocity. Therefore, this is true in conditions where there is an equipartition of kinetic energy between the protons and electrons. In such circumstances, the electron velocities will be much larger due to the electron to proton mass factor. However, proton collisions can be better at redistributing electrons amongst the fine structure levels of a minor species ion. This is principally because the cross-sections for proton induced transitions between levels with small energy separations, can sometimes become sufficient to overcome the low velocity disadvantage. This is also true for transitions between high n-shells because the l-subshells are nearly degenerate.

Collisional Ionisation by Electron Impact / Three Body Recombination

Consider the electron impact ionisation reaction,



This is the direct state resolved total ionisation reaction where the individual electron initial inner shell, ρ , and final target states, τ , are known. It occurs when $\epsilon_1 > \chi_{\tau}$, i.e. the incident electron energy is greater than the ionisation potential of the ion. Alternatively, it can occur through stepwise excitation to an autoionising level, e.g.,



In either case it is described by a reaction cross-section, $\sigma_{\rho \rightarrow \tau} \equiv \sigma_{\tau\rho}$. This in turn can be expressed in terms of the two alternative pathways i.e.

$$\sigma_{\tau\rho} = \sum_{nl} \zeta_{nl} \sigma_{\tau(nl,\rho)} + \sum_i q_{\rho \rightarrow i}^e \quad (2.32)$$

where the $q_{\rho \rightarrow i}^e$ is the excitation rate coefficient to the autoionising level i and ζ_{nl} is the number of electrons in the shell nl i.e. the number of equivalent electrons. $\sigma_{\tau(nl,\rho)}$ is the direct ionisation coefficient from the shell nl . Expression 2.32 assumes that excitation to the level i is always followed by autoionisation. This is not necessarily the case and a modification which omits the second sum in 2.32, to take account of this, is described by Burgess, Summers, Cochrane & McWhirter (1977). Autoionisation can

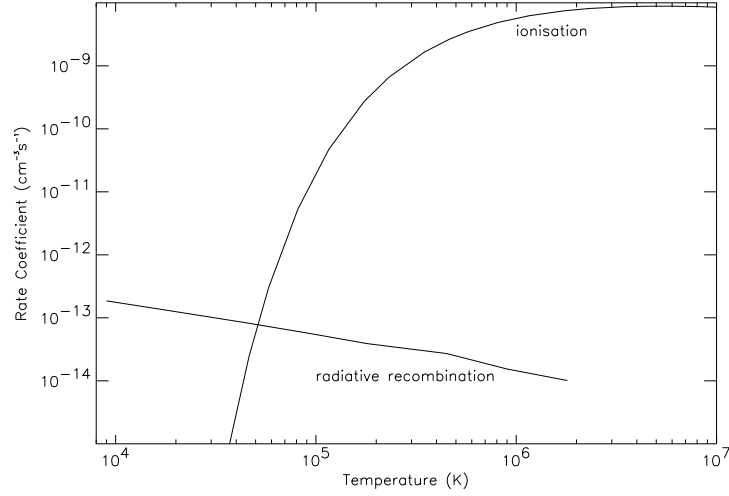


Figure 2.1: Ionisation and Radiative Recombination coefficients for $C^{+2} \leftrightarrow C^{+3}$. Data taken from Abel-Van Maanen(1982)

contribute a substantial amount to the total ionisation cross-section for moderately ionised atoms. For highly ionised systems, the competition with radiative stabilisation means that it is less important. It is described by the radiationless transition probability A^a .

The total ionisation rate coefficient is obtained by integrating over a Maxwellian distribution of electron velocities, i.e.,

$$S_{\tau\rho}^{z \rightarrow z1}(T_e) = 2\sqrt{\pi}\alpha c a_0^2 \left(\frac{kT_e}{I_H}\right)^{1/2} \int_{\frac{I_{\rho\tau}}{kT_e}}^{\infty} \frac{\sigma_{\tau\rho}^{z \rightarrow z1}(\epsilon_{\rho\tau})}{\pi a_0^2} (\epsilon_{\rho\tau}/kT_e) \exp(-\epsilon_{\rho\tau}/kT_e) d(\epsilon_{\rho\tau}/kT_e) \quad (2.33)$$

where $\epsilon_{\rho\tau}$ is the excitation energy separation between the levels ρ and τ . The typical behaviour of an ionisation rate coefficient is illustrated in fig.2.1.

The inverse process in eq. 2.30 is that of three body recombination. The rate coefficient for this process can be obtained from detailed balance, i.e. by equating the reaction rate for ionisation, $N_e N_\rho S_{\tau\rho}^{z \rightarrow z1}$, and the reaction rate for three body recombination, $N_e^2 N_\tau \alpha_{\tau \rightarrow \rho}^3$. Note that three body recombination has a reaction rate proportional to N_e^2 . This effectively means that, although the rate coefficients for this

reaction are generally very small, it becomes the dominant recombination process at very high electron density. Typically this begins to occur at electron densities above $\sim 10^{14} \text{cm}^{-3}$ and becomes more evident as the density increases.

Spontaneous Radiative Decay

Spontaneous radiative decay allows an electron to deexcite from one bound state of an ion, to another bound state of the same ion. This is achieved by the emission of a photon.

$$X_i^z \rightarrow X_j^z + h\nu \quad (2.34)$$

$h\nu$ is the usual term to describe the energy of the emitted photon, and this produces a single spectral emission line at the wavelength corresponding to the frequency ν . As mentioned in sec.2.1.1, the rate coefficient for this reaction is called the transition probability or Einstein coefficient and is denoted by $A_{j \rightarrow i}$. Accurate calculations of them are extremely important as particular transition types have substantially different Einstein coefficients, and this can result in wildly differing relaxation lifetimes (see sec.2.2.2). Consequently, the LTE limit will be approached for some levels much more easily than for others. Three types of transition are generally distinguished.

1. Electric Dipole
2. Non-Dipole
3. Spin changing

Electric dipole transitions have the largest probabilities and these are typically at least 3 \rightarrow 4 orders of magnitude greater than those for non-dipole and spin changing transitions i.e. $\sim 10^7 - 10^{10} \text{s}^{-1}$ compared with $\sim 10^2 - 10^4 \text{s}^{-1}$. For electric dipole transitions the Einstein coefficient can be approximated as,

$$A_{j \rightarrow i} = \frac{16\alpha^4 c}{3\sqrt{3}\pi a_0} \frac{g^I}{n_j n_i (n_i^2 - n_j^2)} \frac{z1^4}{w_j} \quad (2.35)$$

due to McWhirter & Summers (1985), where g^I is the bound-bound Gaunt factor ~ 1 , and the $n_{j(i)}$ represent the effective principal quantum numbers of the level j(i).

As discussed earlier, there is a $z1^4$ dependence. This is true for transitions between principal quantum shells, although the dependence is more like $z1$ for transitions within n shells. The other transition types are much more strongly dependent on $z1$. For type 2 this may be $\sim z1^6 - z1^{10}$ and for type 3 $\sim z1^7 - z1^{10}$, again conditional on whether the transition is within the same n shell, or not. As a result, spectral lines for transitions of types 2 and 3 are much weaker than for type 1 in neutral atoms and near neutral ions, but can become dominant for highly ionised ones.

Finally each of the different transition types are identified by specific quantum mechanical selection rules. For electric dipole transitions, the total orbital angular momentum quantum number L must change by 1. Transitions between levels with different total spin angular momentum S are disallowed and the total angular momentum, quantum number J , cannot change by > 1 . In addition, $J = 0 \rightarrow J = 0$ transitions are forbidden and the parity selection rule stops transitions within configurations. The parity of an excited state is described as *odd* or *even* and can be calculated as $(-1)^{\sum_i l_i}$, where l_i is the angular momentum quantum number of the i th electron. If the result is -1 the parity is odd and this is denoted by a superscript o on the total angular momentum quantum number of the term e.g. P^o . Spin changing transitions take place between levels with different S quantum numbers. This is only possible in relativistic theory, some mention of which is made in sec. 2.2.2. There are a number of different transitions of type 2. Magnetic dipole transitions take place between levels which do not require a change in their total angular momentum. In this case, $\Delta J = 2$ transitions are also forbidden. It is also possible to make an electric quadrupole transition. The electron, in this transition type, must either change its total orbital angular momentum by 2 or not at all. Also, $L = 0 \rightarrow L = 0$ transitions are disallowed.

Radiative Recombination

The radiative recombination reaction is,



where the incident electron loses enough energy, by photon emission, to be captured into some principal quantum shell, n . The recombining ion is sometimes referred to as the *parent* ion. McWhirter & Summers (1985) give an approximate form for the associated radiative recombination coefficient. This is based on the assumption that the energies of the highly excited states are approximately hydrogenic (i.e. degenerate).

$$\alpha_{\rho j}^r = \frac{128}{3} \sqrt{\frac{\pi}{3}} \alpha^4 c a_0^2 z^4 \left(\frac{I_H}{kT_e} \right)^{3/2} \frac{1}{\omega_{nl} n} \exp\left(\frac{\chi_n}{kT_e} \right) \int_{\frac{\chi_n}{kT_e}}^{\infty} \frac{g^{II} \exp(-E/kT_e)}{(E/kT_e)} d(E/kT_e) \quad (2.37)$$

where $j \equiv \rho, nl$ and g^{II} is the bound-free Gaunt factor, which is usually taken to be equal to one. The ionisation energy of the nl shell is χ_{nl} and E is the recombining electron energy. Asymptotically the coefficient behaves like,

$$\begin{aligned} \alpha_{\rho j}^r &\rightarrow \exp(s) Ei(s) \rightarrow 1/s \text{ as } s \rightarrow \infty \\ &\rightarrow -\ln s \text{ as } s \rightarrow 0 \end{aligned} \quad (2.38)$$

where $Ei(s) = \int_s^{\infty} \frac{\exp(-w)}{w} dw$. The first of these is generally more appropriate since the temperature is usually much smaller than the ionisation energy, in an equilibrium plasma (Hutchison (1987)). An example of the typical behaviour of the radiative recombination coefficient is given in fig.2.1. The inverse photon induced processes are not considered in the present context.

Charge Exchange Recombination

The charge transfer reaction takes place between an ion and neutral hydrogen as follows,



where the proton, p , represents singly ionised hydrogen. Generally, the number of neutral hydrogen atoms, with which charge exchange can occur, is much less than the number of electrons. Evidently then, collisional processes involving electrons are much more likely to dominate than charge exchange. In the solar transition region and corona, sufficient numbers of neutral hydrogen atoms are not likely to be present. In contrast, in fusion plasmas, neutral hydrogen beams are actively injected

into the plasma in order to generate heat and also to work as a localised spectroscopic diagnostic. A charge transfer reaction with helium beams is also important in fusion plasmas but, due to the even smaller quantities of the species in the solar atmosphere, it is even less likely to be of importance there.

One effect of charge exchange is to reduce the overall ionisation state of an element. This occurs because the charge exchange recombination coefficient is much larger than the radiative recombination coefficient, and therefore, produces a substantial increase in the total recombination rate. This has consequences for the associated ionisation balance etc. Expressions for charge transfer cross-sections and rate coefficients are dominated by contributions from different physical processes. The change in the relative speeds of the target and projectile species has an influence on the controlling process. For an in depth overview see Janev & Winter(1985) and references therein.

Dielectronic Recombination / Autoionisation

Dielectronic recombination occurs if an incident electron excites an electron in the target parent ion, X_i^{z1} , while simultaneously losing sufficient energy to be captured into a bound state, nl.



Here ρ denotes the metastable states of the parent ion, τ denotes the metastable states of the recombined ion, j is an ordinary excited state and nl is a bound orbital with n and l large. In general, this occurs if the incident electron has an energy slightly less than the excitation energy required. As a result, the condition is inherently unstable and may only be transient. That is, it can easily break-up in an *Auger* reaction which returns the individual electrons to their initial states; the leftward arrow in the first part of eq. 2.40. However, it is possible that the ion will rid itself of its excess energy by emitting a photon before this has time to occur. In that case, the incident free electron is ‘properly captured’ and the ion recombines. The captured electron makes no contribution to the stabilisation phase. The spectrum line associated with the radiated photon is called a *satellite line* and can be useful

for temperature diagnostics. Its wavelength is $\sim \frac{hc}{\Delta E_{\rho j}}$. The two processes in the dielectronic recombination reaction are usually referred to as *resonant capture* and *radiative stabilisation*. The Auger decay is also referred to as *autoionisation* and this has been discussed above.

We can distinguish total and partial zero density dielectronic recombination coefficients. Expressions for these have been given by Burgess(1964,65) and a useful review was presented by Seaton & Storey (1976). Here we follow these authors and express the partial dielectronic recombination coefficient as,

$$\alpha_{\rho k}^d = \frac{\omega_k^z}{\omega_\rho^{z-1}} \frac{h^3}{2(2\pi m_e k T_e)^{3/2}} \sum_{\tau} A_{j,nl \rightarrow \tau, nl} \sum_{nl} \exp\left(\frac{-E}{k T_e}\right) A^{cap} \quad (2.41)$$

where $k \equiv \tau, nl$ and the statistical weight, ω_k^z , is the product of ω_j and ω_{nl} . A^{cap} is the capture cross-section which estimates the probability of dielectronic capture into nl ; taking account of the possibility of autoionisation. It is expressed as,

$$A^{cap} = \frac{\sum_f A_{j,nl \rightarrow \rho, f}^a}{\sum_f A_{j,nl \rightarrow \tau, f}^a + \sum_{\tau} A_{j,nl \rightarrow \tau, nl}} \quad (2.42)$$

where the A^a 's are autoionisation transition probabilities. It is likely that the most efficient dielectronic recombination rate will be obtained when $\rho = \tau$. This is because returning to the initial metastable state means that the final state energy is low enough to avoid the Auger break up reaction (Burgess(1964)). The total dielectronic recombination rate coefficient can be obtained by summing over all possible intermediary states j, nl thus

$$\alpha_{\rho k}^{dtot.} = \sum_{j, nl} \alpha_{\rho k}^d \quad (2.43)$$

These potentially transient states are referred to as *doubly excited*, and the summation extends from the lowest energetically accessible one to infinity. The lowest accessible state corresponds to the case where nl satisfies,

$$E_\rho = E_{\tau, nl} + h\nu \quad (2.44)$$

Only at zero density do all resonant captures cascade to the ground level and contribute to the effective dielectronic recombination coefficient. At increasing density secondary collisional redistribution is more likely to intervene in the process before

radiative stabilisation has had time to occur. At some critical density, collisional ionisation will dominate over radiative stabilisation. The main effect of this is to suppress the dielectronic recombination coefficient at high density. Therefore, dielectronic recombination has a more important role to play in low density plasmas. Burgess(1964) also showed that dielectronic recombination was extremely important in high temperature plasmas. At high temperature, the mean electron energy, kT_e , can be comparable to the resonant excitation energy, ϵ . As a result, the exponential term in eq. 2.41 is much larger than usual and this results in an enhancement in the dielectronic recombination coefficient itself, typically $\sim 10 - 20$ times larger than the radiative recombination coefficient.

In this work we are considering solar plasmas which can be high temperature and low density, for example, the corona. Burgess & Seaton (1964) showed that by including dielectronic recombination they were able to remove the previously existing discrepancy between the coronal temperature deduced from ionisation equilibrium calculations, and the temperature inferred from spectral measurements, e.g. doppler line widths. We should note that dielectronic recombination is now regarded as the dominant recombination process in the solar corona.

2.2.2 Collisional-Radiative Theory

The original concept of Collisional-Radiative modelling was developed by Bates, Kingston & McWhirter (1962). It encompasses both the low density coronal equilibrium approximation and the high density LTE model. It takes full account of the shifting influence of collisional and radiative processes dependent on the electron density and the excitation energy of the principal quantum shell. All radiative and electron collisional processes are included in the model. Photon induced ones e.g. stimulated emission, photoionisation etc., are not.

The ion in the plasma is assumed to consist of a complete set of levels with collisional and radiative couplings between each of them. In addition, direct ‘*state resolved*’ ionisation and recombination coefficients to and from the next ionisation stage are included. The quasi-equilibrium assumption is then invoked to *condense*

the influence of the highly excited states onto the dominant states. In this way effective contributions to the evolution of the dominant populations, from the sub-dominant ones, can be identified. At finite plasma densities these contributions may include direct transitions to the dominant states, but can also include transitions via indirect pathways. Examples of the latter are, recombination into highly excited states followed by recombination cascade or stepwise excitation leading to ionisation. Bates et al. (1962) named these contributions collisional-radiative recombination and ionisation coefficients. Following this, Burgess & Summers (1969) included dielectronic recombination in the specification of the collisional radiative recombination coefficient. This allowed them to introduce *collisional-dielectronic* recombination and ionisation coefficients, which Summers (1973) later extended to be dependent on density as well as temperature. These coefficients give the connection between different ionisation stages. In this work it is these latter coefficients that are used. If the dominant populations include metastable states, the coefficients are said to be *generalised*. Collisional-radiative theory also makes a distinction between levels that exist below the collision limit, and those that do not.

It is worthwhile, as background, to present an outline of the theory which establishes the effective recombination and ionisation coefficients used in the time dependent calculation of the dominant populations. This includes the technique of *population condensation*, referred to earlier, which can be generalised to arbitrary level sets. It is clear that different situations require different modelling approaches. For example, the dominant spectrum line emission tends to come from low-lying levels for which a complete specification of the level structure is required. Conversely for highly excited states a much less detailed description is necessary, perhaps dealing with principal quantum shells only. Chap.3 addresses a number of these issues more completely.

Effective Coefficients and Population Condensation

If we consider an ion X^{+z} with arbitrary levels $1 \leq i, j \leq \infty$ below the continuum and recombining ion X^{+z1} , then the statistical balance equations for the level i are,

$$\begin{aligned}
\frac{dN_i}{dt} = & \sum_{\sigma} N_e N_{\sigma}^{z1} \left(\alpha_i^r + \alpha_i^d + N_e \alpha_i^3 + \left(\frac{N_H}{N_e} \right) \alpha_i^{cx} \right) \\
& + \sum_{j>i} N_j \left(N_e q_{j \rightarrow i}^e + N_e q_{j \rightarrow i}^p + A_{j \rightarrow i} \right) \\
& + \sum_{j<i} N_j \left(N_e q_{j \rightarrow i}^e + N_e q_{j \rightarrow i}^p \right) \\
& - N_i \left(\sum_{j>i} \left(N_e q_{i \rightarrow j}^e + N_e q_{i \rightarrow j}^p \right) \right) \\
& + \sum_{j<i} \left(N_e q_{i \rightarrow j}^e + N_e q_{i \rightarrow j}^p + A_{i \rightarrow j} \right) \\
& + \sum_{\sigma} \left(N_e s_{i \rightarrow \sigma} + A_{i \rightarrow \sigma}^a \right)
\end{aligned} \tag{2.45}$$

where we have included all rate coefficients for the relevant processes in an optically thin low density thermal plasma (see sec.2.1) and we have implicitly assumed that the electron, involved in the four recombination processes, is fully captured although this has not been explicitly noted in the expressions for the α 's. The subscript σ refers to the metastable states of the recombining ion, N_e is the electron density, N_H is the hydrogen density and N_i is the population density of the level i . Let us express eq. 2.45 differently by gathering together the recombination, ionisation, excitation and deexcitation terms and defining them more helpfully i.e.

$$\frac{dN_i}{dt} = \sum_{j \neq i} C_{j \rightarrow i} N_j + \sum_{\sigma} N_e N_{\sigma}^{z1} r_{\sigma i} - \sum_{\sigma} N_i S_{i \sigma} - \sum_{j \neq i} C_{i \rightarrow j} N_i \tag{2.46}$$

The new coefficients are defined as,

$$C_{j \rightarrow i} = A_{j \rightarrow i} + N_e \left(q_{j \rightarrow i}^e + q_{j \rightarrow i}^p \right) \tag{2.47}$$

$$C_{i \rightarrow j} = A_{i \rightarrow j} + N_e \left(q_{i \rightarrow j}^e + q_{i \rightarrow j}^p \right) \tag{2.48}$$

$$r_{i \sigma} = \alpha_i^r + \alpha_i^d + N_e \alpha_i^3 + \left(\frac{N_H}{N_e} \right) \alpha_i^{cx} \tag{2.49}$$

$$S_{\sigma i} = N_e s_{i \rightarrow \sigma} + A_{i \rightarrow \sigma}^a \tag{2.50}$$

This allows us to define a total loss coefficient C_{ii} for the level i , viz.

$$-C_{ii} = C_{i \rightarrow j} + \sum_{\sigma} S_{\sigma i} \quad (2.51)$$

which, combined with the populating term,

$$-C_{ij} = C_{ii} + C_{j \rightarrow i} \quad (2.52)$$

defines the usual collisional-radiative matrix previously used by, amongst others, Summers (1973), Burgess & Summers (1976), Spence (1987) and Dickson (1993). Therefore, we can rewrite eq. 2.46 as,

$$\frac{dN_i}{dt} = \sum_{\sigma} N_e N_{\sigma}^{z1} r_{i\sigma} - \sum_j C_{ij} N_j \quad (2.53)$$

This equation provides us with a mechanism for calculating arbitrary level populations. By substituting for the N_j we can recover the dominant populations N_i , be they ground or metastable states. First we must calculate the N_j . This is readily done by invoking the quasi-equilibrium assumption which allows us to set the left hand side of eq. 2.53 equal to zero. It is clear also that the recombination term could be split to its component parts. It is often usual to do this in order to separate out the contribution due to charge exchange recombination (Summers (1994)).

For simplicity, we will illustrate here, the procedure adopted assuming that only the ground states of the X^{+z} and X^{+z1} ion, are heavily populated. We denote the ground state of the X^{+z} ion by ρ , and the ground state of the parent ion by τ . This approach can be generalised to include the effects of the metastable states in the collisional-dielectronic coefficients (see Dickson (1993), Summers (1994)). As such it introduces the effective metastable cross-coupling coefficients and parent-parent metastable cross-coupling coefficients (see sec.3.2.1).

If we now partition the ground states exclusively out of eq. 2.53, we obtain,

$$\frac{dN_{\rho}}{dt} = - \sum_{j>\rho} C_{\rho j} N_j - C_{\rho\rho} N_{\rho} + N_e N_{\tau} r_{\rho\tau} \quad (2.54)$$

For the quasi-static excited populations we have,

$$\frac{dN_i}{dt} = 0 = - \sum_{j>\rho} C_{ij} N_j - C_{i\rho} N_{\rho} + N_e N_{\tau} r_{\tau i} \quad (2.55)$$

which gives, in equilibrium,

$$N_j^{eq} = - \sum_i C_{ji}^{-1} C_{i\rho} N_\rho + \sum_i C_{ji}^{-1} N_e N_\tau r_{\tau i} \quad (2.56)$$

Substituting into eq. 2.54 we get,

$$\frac{dN_\rho}{dt} = - \left(C_{\rho\rho} - \sum_j \sum_i C_{\rho j} C_{ji}^{-1} C_{i\rho} \right) N_\rho + \left(r_{\rho\tau} - \sum_j \sum_i C_{\rho j} C_{ji}^{-1} r_{\tau i} \right) N_e N_\tau \quad (2.57)$$

This allows us to specify the collisional-dielectronic recombination coefficient,

$$\alpha_{CD} = r_{\rho\tau} - \sum_j \sum_i C_{\rho j} C_{ji}^{-1} r_{\tau i} \quad (2.58)$$

and the collisional-dielectronic ionisation coefficient,

$$S_{CD} = \left(C_{\rho\rho} - \sum_j \sum_i C_{\rho j} C_{ji}^{-1} C_{i\rho} \right) / N_e \quad (2.59)$$

so that the time dependent equation for the ground state ρ finally becomes,

$$\frac{dN_\rho}{dt} = N_e N_\tau \alpha_{CD} - N_e N_\rho S_{CD} \quad (2.60)$$

These coefficients are now density dependent also and include contributions from their simpler temperature dependent individual reaction forms. The method of assuming a quasi-static situation for the excited states and solving for the dominant populations, is the explanation for the term condensation. In principal, this excited state partition could take place anywhere, although it is usual to keep this decision on a firm physical basis. The effective coefficients provide a measure of the influence of the highly excited levels, projected onto the low lying ones. As such, they provide convenient parameters for data storage which can be throughput to dynamical transport models.

Metastable states

Metastable states have been briefly mentioned above, but it is helpful at this stage, to provide an explicit example. If we adopt the commonly used Russell-Saunders, or LS, coupling scheme, then there are quantum mechanical selection rules which

decide what spontaneous radiative transitions are possible. Mention of these was briefly made in sec.2.2.1. The net effect of these is to promote or inhibit a particular transition and these are generally termed *allowed* or *forbidden*. In general, a state becomes metastable if it is forbidden to decay easily to the ground state. This may arise if it has to decay via a *non-electric dipole* transition. As we have seen, in LS coupling, a change in the *total spin angular momentum*, quantum number S , is not allowed. Therefore, *exchange* transitions between different spin systems are forbidden. More specifically, the selection rule disallows $\Delta S \neq 0$ transitions. In addition, transitions between the same configurations are forbidden by the parity selection rule. Metastable states will form if they have to break either of these rules to make a transition to the ground state.

Fig. 2.2 shows the Grotrian diagram of Be-like C^{+2} for transitions amongst the twelve lowest lying levels. These include some $n = 2 \rightarrow 3$ transitions. The left hand side of the diagram identifies the levels that occur in the singlet spin system, while the right hand side shows those from the triplet system. It is easily seen that the only metastable term for Be-like ions is that of the $1s^2 2s 2p \ ^3P$, due to its inability to decay from the triplet spin system. There is no metastable term in the singlet system as electrons can cascade quite freely to the $1s^2 2s 2p \ ^1P$ term, which has an electric dipole pathway to the ground. This inability of metastable states to relax, allows them to collect populations which may be of the same order as that of the ground level. We have already seen that their lifetimes can be comparable to that of the ground level, so it is clear that they must be identified and modelled dynamically in the plasma transport equations. The complete set of metastable states for oxygen is presented in chap.4 sec.4.3.1. This partition holds true also for all H-like to O-like ions.

In relativistic theory it is possible for metastable states to relax more freely. This occurs because it is necessary to take account of spin-orbit interactions in the Hamiltonian. The latter is done by adding a spin-orbit term as a perturbation to the electrostatic Hamiltonian, producing the Breit-Pauli Hamiltonian (see Berrington, Eissner & Norrington (1995)). When these perturbations are non-negligible, LS coupling breaks down into intermediate coupling. The perturbations split the LS terms

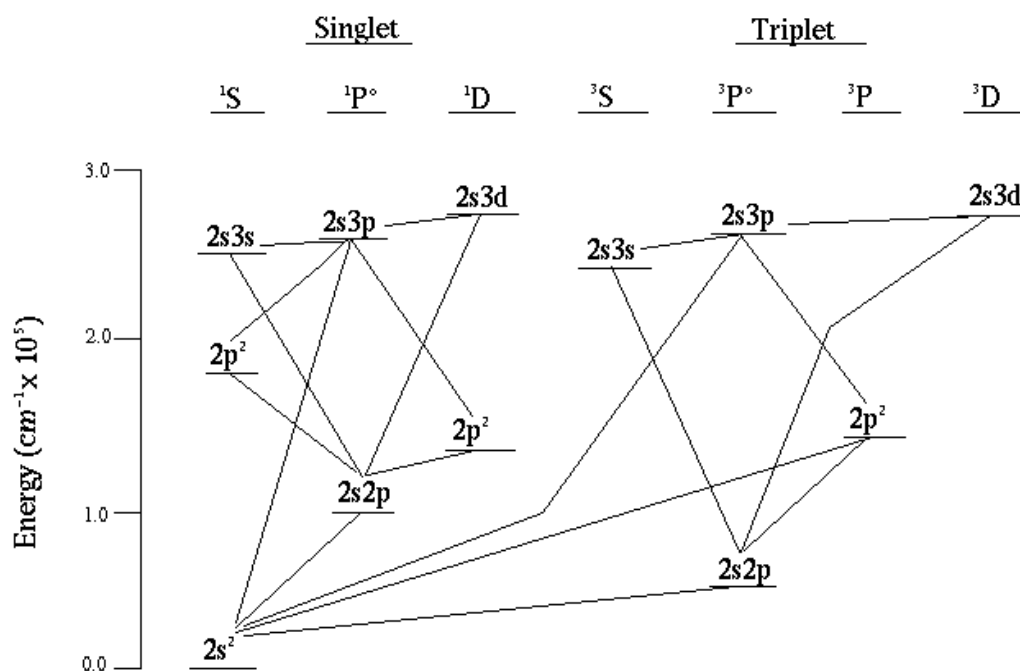


Figure 2.2: Grotrian Diagram for Be-like CIII

into fine structure levels, according to their J quantum numbers. It is then possible for intersystem transitions, via the J-resolved levels, to allow the metastables to decay to the ground. For example, an intercombination transition from $2s2p\ ^3P_1$ to the $2s^2\ ^1S_0$ ground level becomes weakly allowed. Also, a magnetic quadrupole transition from $2s2p\ ^3P_2$ to the ground becomes active.

2.2.3 Derived Atomic Data and their Application to Spectroscopic Diagnostics

In order to gain understanding of the behaviour of plasmas it is important to develop methods for diagnosing their properties. In laboratory plasmas, powerful techniques are in use to measure parameters such as electron density and temperature. These can involve passing laser beams into the plasma to measure the backscattered light (LIDAR - LIght Detection And Ranging) or to compare the beam with one that traverses the same distance, but not through the plasma (infra red interferometry). See Dickson (1993) for a discussion. In addition, placing magnetic probes in the plasma or attaching particle samplers to the plasma container walls, are extremely useful techniques for investigating magnetic field geometry and strength and for diagnosing temperature and density, respectively. Acquiring diagnostic information through spectroscopy is commonplace, but it is rarely necessary to rely solely on the radiation emission to infer plasma parameters and the physical processes at work. For example, neutral beam injection also provides information on the magnetic field through Stark splitting due to the electric field and a prior knowledge of the beam velocity (Wolf (1993)), but this is mainly used with known electron densities and temperatures to diagnose the physical processes at work.

The high temperature solar corona is optically thin. Therefore, radiation is one of the main energy loss mechanisms from the solar upper atmosphere. Here, it is essential to calculate radiation signatures observable by spectroscopic instrumentation. Current technology makes it impractical to consider releasing a solar probe into the hostile environment. Therefore, in remote sensing of the solar atmosphere the only potential diagnostic information we can obtain is this radiation.

We should be aware of the potential limitations of this approach. For example, the intensity of a spectral line emitted by a column of optically thin plasma resulting from a transition $i \rightarrow j$ is formally expressed as

$$I_{i \rightarrow j} = \int \int k(T_e, N_e) \phi(T_e, N_e) dT_e dN_e \quad (2.61)$$

The $\phi(T_e, N_e)$ function is the emission measure differential in temperature and density and represents the most information on the plasma that we can obtain without making any more assumptions. The $k(T_e, N_e)$ is the kernel function which contains the contribution function and the elemental abundance. Recent work by Hubeny & Judge (1995) and Judge, Hubeny & Brown (1997) has shown that the information content of the spectrum is very small and that, due to the ill posed nature of the problem, it is extremely difficult to infer anything about the temperature and density structure of the plasma given the errors associated with the observations and the kernel functions. Indeed, they suggest that with realistic errors information on the density dimension becomes lost in the spectral data noise, making it unrealistic to expect to determine density distributions in addition to temperature distributions.

The usual approach in the astrophysics community has been to proceed by making a number of simplifying assumptions about the nature of the plasma under investigation until eventually arriving at the formulation of Eq.2.62.

$$I_{i \rightarrow j} = \frac{1}{4\pi} \frac{N_{tot}}{N_H} \int_{t_1}^{t_2} G_{i \rightarrow j}(T_e, N_e) \phi(T_e) dT_e \quad (2.62)$$

where $\frac{N_{tot}}{N_H}$ is the abundance of the element, $\phi(T_e)$ is the emission measure differential in temperature and the limits t_1 and t_2 represent the two temperature extremes of the plasma volume contributing to the line. The assumptions are as follows. The elemental abundance is assumed constant over the plasma depth. This allows us to separate the kernel function into the abundance, $\frac{N_{tot}}{N_H}$, and the contribution function ($G(T_e, N_e)$). The abundance is subsequently taken outside of the intensity integral. Here we have also explicitly noted the slight dependence of the contribution function on density. The plasma pressure is assumed constant over the temperature width of significant values of the $G(T_e, N_e)$ function. This method assumes a relationship between temperature and density, allowing us to change the variable of the integral

from the viewing volume to the electron temperature (Craig & Brown (1976)). Therefore, under these simplifications, we avoid the bi-variate integral dependent also on density and the $G(T_e, N_e)$ function can be assumed effectively dependent only on temperature. Finally, the function $\phi(T_e)$ is the average value of the differential emission measure over the viewed region and tells us something about the structure of the atmosphere at the temperature T_e . It is mathematically equivalent to the integral of the differential emission measure in density i.e.

$$\phi(T_e) = \int \phi(T_e, N_e) dN_e \quad (2.63)$$

If we have a series of line intensity observations and their corresponding $G(T_e, N_e)$ functions, we can attempt to invert the integral (2.62) to obtain the differential emission measure. Many inversion algorithms have been developed to do just this (Harison & Thompson (1992)). As mentioned above, it is extremely difficult to produce meaningful results in the bi-variate case and the solution for the temperature dependent case is of limited value. (See chapter.5 for a discussion on the differential emission measure in temperature and its validity with regard to the solar atmosphere).

The predictive approach is more secure. If we have a plasma model we can produce a $\phi(T_e, N_e)$ function and combine it with calculations of $G(T_e, N_e)$'s to predict spectral line intensities. These can then be compared to the observations. In this way, we can gain physical insight into the processes which contribute to the formation of the individual spectral line intensities. Consequently, we can refine our theoretical models and attempt, ultimately, to match the observations. Note that a complete match will only ever tell us that our model provides one possible solution to the problem, not that it is correct.

Whichever approach is used, the line emission contribution function is required and this is expressed as,

$$G_{i \rightarrow j}(T_e, N_e) = A_{i \rightarrow j} \frac{N_H}{N_e} \sum_{\sigma=1}^{m_z} \frac{N_i^z}{N_e N_\sigma^z} \Big|_{q.s.} \frac{N_\sigma^z}{N_{tot}^z} \Big|_{eq.} \quad (2.64)$$

where $A_{i \rightarrow j}$ is the spontaneous transition probability for the transition $i \rightarrow j$, N_H is the hydrogen density and N_e is the electron density. $\sum_{\sigma=1}^{m_z} \frac{N_i^z}{N_e N_\sigma^z}$ represents the collisional-radiative calculation of the population dependence of the level, i , on the

metastables of the ionisation stage, z . This is computed in the quasi static approximation (see sec.2.2.2) and assumes that effective contributions to the population of the level i come only by excitation from the metastables, such that,

$$N_i^z = \sum_{\sigma=1}^{m_z} N_e N_\sigma^z f_{i \rightarrow \sigma}^{exc}. \quad (2.65)$$

The final part of eq. 2.64 describes the population distribution of the different ionisation stages using the assumption of equilibrium. It is possible to include a time dependent calculation here but this would be dependent on a temporal model and consequently would restrict the applicability of the contribution function and the differential emission measure. The temperature corresponding to the peak of the ionisation stage curves is often used as an estimate of the formation temperature for spectral lines emitted by an ion. An exploration of the influence of metastable states on the ionisation balance is conducted in chap.4.

The ‘derived’ quantities we refer to here, are calculated from the fundamental atomic collision cross-sections by taking account of level population density and collisional-radiative effects. Therefore, on final computation, they may be model dependent. Contribution functions ($G(T_e, N_e)$ functions) and equilibrium ionisation stage populations are included and photon emissivity coefficients are another example. Leaving aside problems associated with the spectrometer interpretation, e.g. errors in the intensity calibration, we can establish theoretical expressions that we can couple with our models to confront the spectral measurements.

In the astrophysics community it has often been the case that line intensity ratios are used as diagnostics of plasma density and temperature. For estimates of electron temperature, two lines which are sensitive to temperature are chosen. Then, the assumption is made that the temperature of the plasma is uniform over the region of emission. In theory this allows us to take the $G(T_e, N_e)$ function outside the integral in eq. 2.62, so that the intensity ratio becomes a ratio of excitation coefficients only, i.e.,

$$\frac{I_{i \rightarrow j}}{I_{k \rightarrow l}} = \frac{q_{g \rightarrow i}}{q_{g \rightarrow k}} \quad (2.66)$$

The excitation rate coefficients are not ‘derived’ in the same sense as described above

but are model dependent in that it is assumed that the distribution of electron velocities in the plasma is Maxwellian. Bearing this in mind we can proceed to recover a plasma temperature. The physical meaning of this temperature is probably obscured by the assumptions involved in the derivation. As pointed out by Lang, Mason & McWhirter (1990) the formulation of eq. 2.62 has already implicitly assumed something about the temperature dependence, for example, through the ionisation balance. It is also based on the assumption that the atmosphere is composed of concentric surfaces of constant temperature and pressure. Hubeny & Judge (1995) state that it is simply "the single temperature of an isothermal plasma that reproduces the observed intensity ratio". Whether the plasma is indeed isothermal is open for debate. Also, the technique may be uncertain due to the dependence on the ionisation balance fractions used. Therefore, it is more appropriate to consider the ratio between lines as being that between the full integrals of eq. 2.62. Evidently, the ratio is then independent of the abundance and is usually fairly insensitive to the ionisation balance calculations. As a result, moderate uncertainties in the technique can be partially removed.

For estimates of electron density it has been usual to take the ratio between lines, one of which arises from a metastable. Since metastables are collisionally disrupted, above some critical density, the ratio will also be sensitive to electron density. Collisional deexcitation of the metastables is much faster than radiative decay so lines originating from a metastable become more intense. Conversely, transitions terminating in a metastable have associated lines which are weaker. Eq. 2.66 is usually used for this also, except that the excitation coefficients are now density dependent. Our earlier assumption of constant pressure ensures that this line ratio technique can be used but once again the physical interpretation of the result is uncertain. Indeed, the work of Judge et al.(1997), mentioned above, implies that the inferred density is likely to be wrong and that more information on the structure being observed is needed to go any further. Nevertheless, line ratio techniques are still in widespread use. Order of magnitude estimates of plasma parameters can be useful in some circumstances, although more detailed studies are likely to benefit only from a predictive modelling approach. Clearly, the applications of the $G(T_e, N_e)$ function are widespread. For

astrophysical work it is of use to archive them at a range of plasma pressures, for use in differential emission measure and line ratio analyses.

Since it is often the line intensity that is required for observational comparison, we might ask whether mass production and collection of these is appropriate. In general, this is less helpful since they depend on both the metastable state populations of the individual ionisation stage, and also the stage to stage ionisation balance. The former may be computed from the quasi-equilibrium assumption and effective contributions to the dominant populations (see eq. 2.56) archived. This assumption is justified and is assured when an initial model for the dominant populations is specified. The assumption of ionisation balance is less secure. Generally it requires some model assumption about the nature of the plasma under investigation. It is probably more appropriate to treat this point as a reasonable cut-off between the calculation of purely fundamental atomic parameters, and subsequent model dependent data. In this work we treat photon emissivity coefficients as an intermediary class of data which facilitates the transfer from pure to applied data. These are temperature and density dependent (i.e. they are also derived) but are appropriate for archiving over suitable temperature and density ranges that are applicable to solar and fusion studies.

It is possible to identify photon emissivity coefficients for each process by extracting their contribution to the evolution of the dominant populations from eq. 2.65 (e.g. as in eq. 2.56 and see Summers et al.(1996) for a complete description). We can derive an expression for the line emissivity which allows us to pick out the photon emissivity coefficients. This proceeds as follows. If the line emissivity for a transition $i \rightarrow j$ is given by,

$$\epsilon_{i \rightarrow j} = A_{i \rightarrow j} N_i \quad (2.67)$$

then using eq. 2.65, with individual reaction components included, we get,

$$\epsilon_{i \rightarrow j} = A_{i \rightarrow j} \left(\sum_{\sigma=1}^{m_z} N_e N_{\sigma}^z f_{i \rightarrow \sigma}^{(exc)} + \sum_{\tau=1}^{m_{z+1}} N_e N_{\tau}^{z+1} f_{\tau \rightarrow i}^{(rec)} + \sum_{\tau=1}^{m_{z+1}} N_H N_{\tau}^{z+1} f_{\tau \rightarrow i}^{(cx)} + \sum_{\rho=1}^{m_{z-1}} N_e N_{\rho}^{z-1} f_{\rho \rightarrow i}^{(ion)} \right) \quad (2.68)$$

where the f's are effective contributions to the population of the excited state i due to excitation from the metastables, recombination from the parent ion, charge exchange

recombination from neutral hydrogen and ionisation from the $z - 1$ ion. ρ, σ and τ index the metastable states of the $z - 1, z$ and $z + 1$ ions respectively. As a result the photon emissivity coefficients are defined as,

$$\mathcal{P}\mathcal{E}\mathcal{C}_{\sigma,i \rightarrow j}^{(exc)} = \frac{(A_{i \rightarrow j} f_{i \rightarrow \sigma}^{(exc)})}{N_e} \quad (2.69)$$

for excitation

$$\mathcal{P}\mathcal{E}\mathcal{C}_{\tau,i \rightarrow j}^{(rec)} = (A_{i \rightarrow j} f_{\tau \rightarrow i}^{(rec)}) \quad (2.70)$$

for recombination

$$\mathcal{P}\mathcal{E}\mathcal{C}_{\tau,i \rightarrow j}^{(cx)} = (A_{i \rightarrow j} f_{\tau \rightarrow i}^{(rec)}) \quad (2.71)$$

for charge exchange recombination

$$\mathcal{P}\mathcal{E}\mathcal{C}_{\rho,i \rightarrow j}^{(ion)} = (A_{i \rightarrow j} f_{\rho \rightarrow i}^{(ion)}) \quad (2.72)$$

for ionisation. Examples of the behaviour of such coefficients are provided in chap.4.